IOPscience iopscience.iop.org

Home Search Collections Journals About Contact us My IOPscience

# Charge transfer luminescence of $Yb^{3+}$ ions in $LiY_{1-x}Yb_xP_4O_{12}$ phosphates

This article has been downloaded from IOPscience. Please scroll down to see the full text article.

2007 J. Phys.: Condens. Matter 19 036202

(http://iopscience.iop.org/0953-8984/19/3/036202)

View the table of contents for this issue, or go to the journal homepage for more

Download details:
IP Address: 129.252.86.83
The article was downloaded on 28/05/2010 at 15:21

Please note that terms and conditions apply.

INSTITUTE OF PHYSICS PUBLISHING JOURNAL OF PHYSICS: CONDENSED MATTER

J. Phys.: Condens. Matter **19** (2007) 036202 (12pp) doi:10.1088/0953-8984/19/3/036202

# Charge transfer luminescence of $Yb^{3+}$ ions in $LiY_{1-x}Yb_xP_4O_{12}$ phosphates

**G Stryganyuk[1,2], S Zazubovich[3], A Voloshinovskii[2], M Pidzyrailo[2], G Zimmerer[4], R Peters[5] and K Petermann[5]**

[1] HASYLAB at DESY, Notkestraße 85, 22607 Hamburg, Germany
[2] Ivan Franko National University of Lviv, 8 Kyryla i Mefodiya Street, 79005 Lviv, Ukraine
[3] Institute of Physics, University of Tartu, Riia 142, Tartu 51014, Estonia
[4] Institute of Experimental Physics, University of Hamburg, Luruper Chaussee 149, 22761 Hamburg, Germany
[5] Institute of Laser Physics, University of Hamburg, Luruper Chaussee 149, 22761 Hamburg, Germany

Received 28 September 2006
Published 5 January 2007
Online at stacks.iop.org/JPhysCM/19/036202

**Abstract**

Spectral-kinetic studies have been performed for $LiY_{1-x}Yb_xP_4O_{12}$ ($x = 0$; 0.1; 0.9) phosphates at $T = 8$–320 K using synchrotron radiation for excitation within the 5–17 eV energy range. Mechanisms for the excitation of $Yb^{3+}$ charge transfer and f–f luminescence are discussed. The quasimolecular character of $Yb^{3+}$ charge transfer luminescence (CTL) is pointed out. The central $Yb^{2+}$ ion and hole delocalized over the surrounding ligands are proposed for consideration as a '*charge transfer cluster*' ($Yb^{2+}$ CT cluster). Possible mechanisms of $Yb^{3+}$ CTL quenching are presumed.

## 1. Introduction

Charge transfer (CT) luminescence processes involving trivalent rare earth ions ($RE^{3+}$) have not been widely considered until the last few years. Interest in $Yb^{3+}$ CT luminescence has been renewed after the discovery of possible applications of Yb-containing compounds in the real-time spectroscopy of solar neutrinos [1]. For the first time this phenomenon was observed for $Yb^{3+}$ ions in phosphates and oxysulfides [2, 3]. Charge transfer luminescence has also been reported for $Ce^{4+}$ ions in $Sr_2CeO_4$ [4]. Comprehensive studies of $Yb^{3+}$ charge transfer luminescence in phosphate, borate, aluminate, oxysulfide, oxyhalogenide, oxide and fluoride matrices have been carried out in [5]. The luminescence characteristics of $Yb^{3+}$ doped garnets and perovskites were investigated in [6–8]. Variation of the CT absorption energy for lanthanide ions in a wide variety of host compounds has been studied in [9]. Yb-doped compounds are extensively studied as promising materials for use in neutrino detectors and fast scintillators [8–12].

In case of $RE^{3+}$ ions the charge transfer occurs as an electron transition from a ligand to the impurity $RE^{3+}$ ion. After electron transfer to $RE^{3+}$ the hole appears to be distributed over

 © 2007 IOP Publishing Ltd Printed in the UK 

the ligands around the $RE^{2+}$ ion. When discussing the relaxation of the $Yb^{3+}$ CT state one should take into account that the $RE^{2+}$ ion is formed after electron transfer, and 4f states of $RE^{3+}$ can be realized only after the escape of an electron from $RE^{2+}$. This may occur via the recombination of an electron at $RE^{2+}$ with the hole localized on a ligand. Such recombination can be radiative, giving rise to charge transfer luminescence (CTL).

The redistribution of charge density around impurity $RE^{2+}$ ions occurs after electron transfer, making it difficult to consider the further relaxation of such a $RE^{2+}$ centred system in the framework of a band model. Ion displacement may occur due to the interaction of polarized ligands with the central $RE^{2+}$ ion. This may be the reason for the characteristic large Stokes shift (up to 2 eV) for CTL [9]. It makes sense to consider the formation involving the central $RE^{2+}$ ion and the hole delocalized over the surrounding ligands as a '*charge transfer cluster*'. CTL has a quasimolecular character and it is possibly better to use the cluster approach [13–15] to explain relaxation processes involving $RE^{3+}$ CT state while the CT absorption can be considered using the band model.

Charge transfer absorption may compete with the transitions within the $RE^{3+}$ 4f shell or interconfigurational $4f^n \rightarrow 4f^{n-1}5d$ transitions. In the case of the $Yb^{3+}$ ion the energy of charge transfer is sufficiently different from the energies of $Yb^{3+}$ $4f^{13} \rightarrow 4f^{13}$ and $4f^{13} \rightarrow 4f^{12}5d$ transitions [16]. Thus, there is no competition between these processes and one may observe the intense VUV–UV absorption peaks corresponding to the electron transfer from the ligand to the $Yb^{3+}$ ion. It is possible to realize the $Yb^{3+}$ ground $^2F_{7/2}$ and excited $^2F_{5/2}$ states after the recombination of an electron at $Yb^{2+}$ with the hole localized on the ligand. If such recombination appears to be radiative then two emission bands of $Yb^{3+}$ CTL may be observed. The distance between two maxima of $Yb^{3+}$ CTL corresponds to the energy difference (1.24 eV) between $Yb^{3+}$ $^2F_{5/2}$ and $^2F_{7/2}$ states.

The CTL of $Yb^{3+}$ ions in $LiY_{1-x}Yb_xP_4O_{12}$ ($x = 0.1;\ 0.9$) phosphates has been investigated in the present work. These compounds were chosen because of the low concentration quenching of the emission of $RE^{3+}$ ions in a $LiYP_4O_{12}$ matrix due to the relatively large distance between the nearest $Y^{3+}$ ions (~5.5 Å), thus reducing the probability of nonradiative losses [17]. The highest efficiency of $Nd^{3+}$ $4f^25d \rightarrow 4f^3$ emission in $LiY_{1-x}Nd_xP_4O_{12}$ stoichiometric phosphors has been reached at $x = 0.8$ [18]. Thus, reduced concentration quenching was also expected for the CTL of $Yb^{3+}$ ions in $LiY_{1-x}Yb_xP_4O_{12}$ phosphors with a concentration of $Yb^{3+}$ up to $x = 1$.

## 2. Experimental details

Polycrystalline samples of $LiY_{1-x}Yb_xP_4O_{12}$ ($x = 0;\ 0.1;\ 0.9$) were grown using the melt-solution technique. The luminescent-kinetic studies were performed using synchrotron radiation from the DORIS storage ring at the Deutsches Elektronen Synchotron (DESY, Hamburg) and the SUPERLUMI station facility at HASYLAB [19]. The measurements were carried out within the temperature range 8–320 K. Emission spectra were measured with a resolution of 0.25–5 nm within a 250–1050 nm range using an ARC 'Spectra Pro 308' 30 cm monochromator-spectrograph in a Czerny–Turner mounting equipped with Princeton Instruments CCD detector. Luminescence excitation spectra were scanned with a resolution of 3.2 Å within the range 5–17 eV using a 2 m primary monochromator in a 15° McPherson mounting and a Hamamatsu R6358P photomultiplier at the secondary ARC monochromator. The luminescence decay kinetics was registered within a 200 ns time gate defined by the excitation pulse repetition upon the storage ring operation in five-bunch mode.

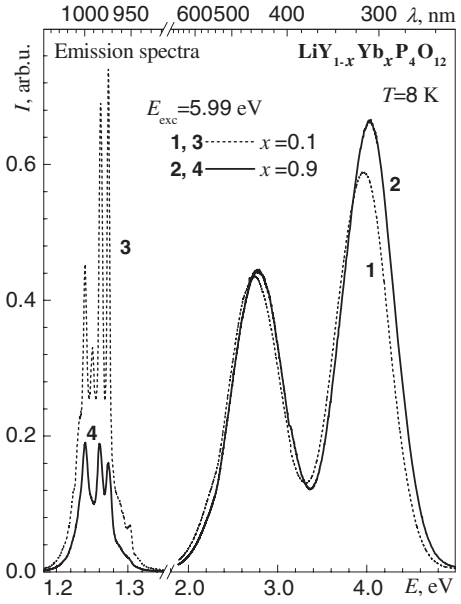


**Figure 1.** Emission spectra of $LiY_{1-x}Yb_xP_4O_{12}$ ($x = 0.1$; 0.9) at $T = 8$ K.

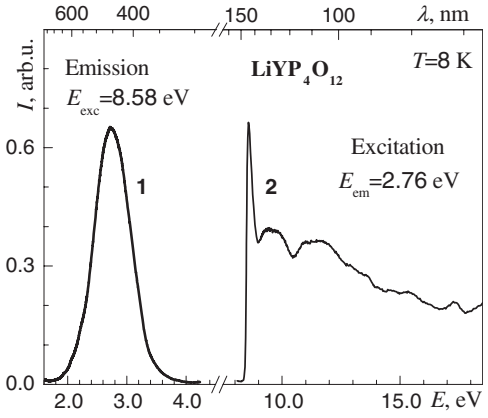


**Figure 2.** Emission (1) and excitation (2) spectra of the intrinsic luminescence of $LiYP_4O_{12}$ at $T = 8$ K.

## 3. Experimental results and discussion

### *3.1. Characteristics of $Yb^{3+}$ charge transfer luminescence*

Upon the excitation of $LiY_{1-x}Yb_xP_4O_{12}$ ($x = 0.1$; 0.9) samples within 5.5–17 eV two broad emission bands were registered in the UV–visible (2.0–4.8 eV) range (figure 1, curves 1, 2) together with the characteristic infrared f–f emission of $Yb^{3+}$ around 1.2–1.3 eV (curves 3, 4).

The low-energy UV–visible band (maximum around 2.8 eV) in the emission spectra of Yb-doped samples (figure 1, curves 1, 2) coincides with the band of intrinsic self-trapped exciton (STE) emission of pure $LiYP_4O_{12}$ (figure 2, curve 1). The excitation spectrum of $LiYP_4O_{12}$ intrinsic emission (figure 2, curve 2) has a threshold around 8.4 eV and a maximum at 8.55 eV corresponding to the excitonic absorption. The decay kinetics is long, possessing the time constant $>10$ $\mu$s at 8 K. From the excitation spectrum of STE emission the band gap $E_g$ can be roughly estimated for $LiYP_4O_{12}$ to be about 8.8 eV.

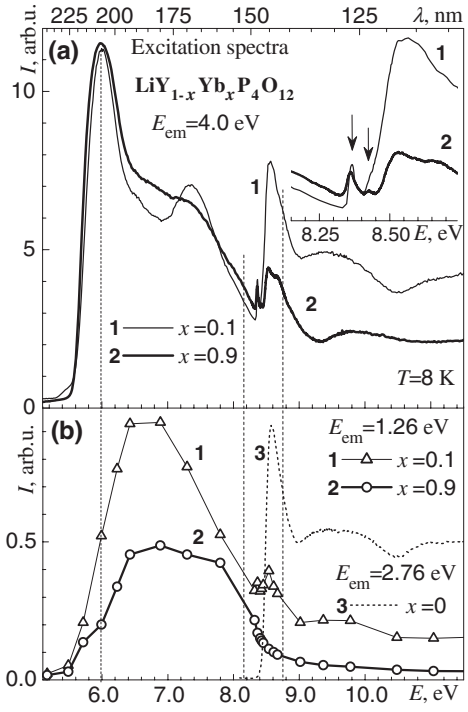


**Figure 3.** Excitation spectra of $Yb^{3+}$ CT and f–f emission for $LiY_{1-x}Yb_xP_4O_{12}$ ($x = 0.1; 0.9$) at $T = 8$ K. To plot the dependences of $Yb^{3+}$ f–f excitation efficiency ((b) curves 1, 2) the integration of $Yb^{3+}$ f–f emission spectra has been performed within the 1.17–1.34 eV range for each value of the excitation energy.

The excitation spectra are similar for both UV–visible emission bands of $LiY_{1-x}Yb_xP_4O_{12}$ ($x = 0.1; 0.9$) samples and show the main maximum around 5.99 eV at 8 K (figure 3(a), curves 1, 2). The distance between two maxima of UV–visible emission bands is about 1.24 eV for both $LiY_{0.9}Yb_{0.1}P_4O_{12}$ and $LiY_{0.1}Yb_{0.9}P_4O_{12}$ samples (figure 1, curves 1, 2). This value is well matched with the energy of $Yb^{3+}$ $^2F$ term splitting. The decay kinetics of UV–visible emission (figure 4) reveals the exponential dependence with a time constant of 160 ns ($LiY_{0.9}Yb_{0.1}P_4O_{12}$, curve 1) and 100 ns ($LiY_{0.1}Yb_{0.9}P_4O_{12}$, curve 5) for the main decay component upon the excitation with a peak of 5.99 eV at 8 K. These decay time values are close to those reported in [2, 3] for the $Yb^{3+}$ CT luminescence of $LuPO_4$:Yb and $YPO_4$:Yb at low temperatures.

Spectral-kinetic characteristics of UV–visible emission observed for $LiY_{1-x}Yb_xP_4O_{12}$ ($x = 0.1; 0.9$) samples allow us to attribute the emission to $Yb^{3+}$ charge transfer luminescence (CTL). Thus, the 5.99 eV peak in the excitation spectra (figure 3(a), curves, 1, 2) corresponds to $Yb^{3+}$ CT absorption, implicating the electron transfer from $O^{2-}$ ligand to $Yb^{3+}$ ion in $LiY_{1-x}Yb_xP_4O_{12}$ ($x = 0.1; 0.9$).

The relatively large (100–160 ns) decay time for the fully allowed CT transitions may be explained by the small overlap of the wavefunctions of the electron at $Yb^{2+}$ and the hole delocalized over $O^{2-}$ ligands [10]. The decrease of the decay time constant for the $LiY_{0.1}Yb_{0.9}P_4O_{12}$ sample may be caused by the nonradiative decay of $Yb^{3+}$ CT states due to concentration quenching.

Upon excitation at 5.99 eV the respective emission bands of $Yb^{3+}$ CTL have an almost equal intensity for both $LiY_{1-x}Yb_xP_4O_{12}$ ($x = 0.1; 0.9$) samples (figure 1, curves 1, 2). The only exception is the difference in the high-energy band peaked around 4.0 eV where the $LiY_{0.1}Yb_{0.9}P_4O_{12}$ sample reveals a slightly higher intensity. The high-energy emission band of $Yb^{3+}$ CTL is more intense for both Yb-doped samples. The intensity ratio for two

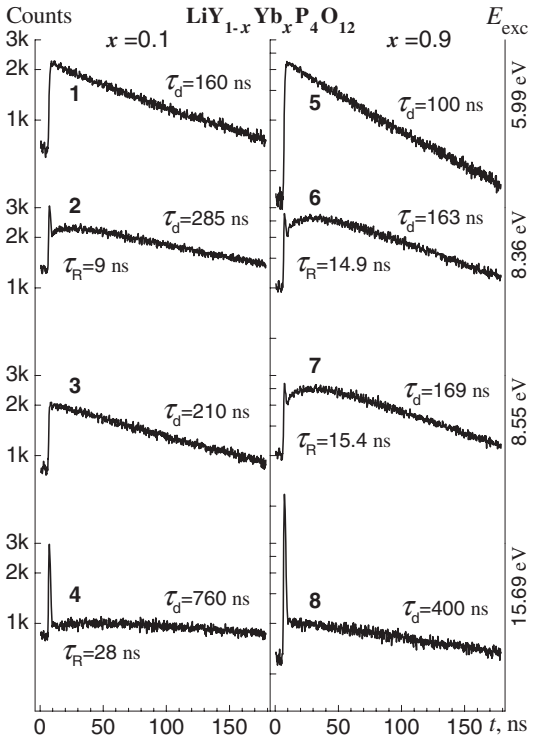


**Figure 4.** Decay kinetic curves for the $Yb^{3+}$ CT emission of $LiY_{1-x}Yb_xP_4O_{12}$ ($x = 0.1$; 0.9) upon the different excitations at $T = 8$ K.

CTL bands is 1.35 for $LiY_{0.9}Yb_{0.1}P_4O_{12}$ and 1.49 for $LiY_{0.1}Yb_{0.9}P_4O_{12}$. These ratio values are constant upon excitation in the 5.6–17 eV range at $T = 8$–320 K. One may conclude the different probabilities of realization of $Yb^{3+}$ $^2F_{5/2}$ and $^2F_{7/2}$ states for $LiY_{0.9}Yb_{0.1}P_4O_{12}$ and $LiY_{0.1}Yb_{0.9}P_4O_{12}$ samples after $Yb^{2+}$ CT cluster decay. The higher ratio (1.49) for the $LiY_{0.1}Yb_{0.9}P_4O_{12}$ sample may imply the higher probability for the radiative relaxation of $Yb^{2+}$ CT cluster down to the $Yb^{3+}$ $^2F_{7/2}$ state. The lower intensity of $Yb^{3+}$ f–f emission can be regarded as a consequent result for the $LiY_{0.1}Yb_{0.9}P_4O_{12}$ sample (figure 1, curve 4) upon excitation in the 5.6–17 eV range. However, concentration quenching may also have an effect in the decrease of $Yb^{3+}$ f–f emission for such a high concentration ($x = 0.9$) of $Yb^{3+}$ ions.

### *3.2. Characteristics of $Yb^{3+}$ f–f luminescence*

The infrared $Yb^{3+}$ f–f emission is about three times more efficient for the $LiY_{0.9}Yb_{0.1}P_4O_{12}$ sample upon excitation at 5.99 eV (figure 1, curves 3, 4). Lines in the infrared emission spectra of $Yb^{3+}$ $^2F_{5/2}$–$^2F_{7/2}$ are rather broad for both Yb-doped samples. This may occur due to some disorder in position of the impurity ion.

Maximum of the excitation efficiency for $Yb^{3+}$ $^2F_{5/2}$–$^2F_{7/2}$ infrared emission has been registered around 6.7 eV for both Yb-doped samples (figure 3(b), curves 1, 2). To plot the excitation spectra for $Yb^{3+}$ f–f emission the luminescence spectra measured upon the corresponding excitation were integrated within the 1.17–1.34 eV range. It is not quite clear why the maximum in the excitation spectra of $Yb^{3+}$ f–f emission (6.7 eV) does not coincide with the $Yb^{3+}$ CT absorption peak (5.99 eV). Interconfigurational $Yb^{3+}$ $4f^{13} \rightarrow 4f^{12}5d$ absorption transitions may also give rise to $Yb^{3+}$ $4f^{13} \rightarrow 4f^{13}$ infrared emission, but they are expected in the higher energy range (8.5–10 eV). A possible explanation may

be based on the presence of the different competing branches for the transformation of the excitation energy. One cannot exclude the defect origin of the 6.7 eV excitation peak observed for $Yb^{3+}$ infrared emission. The defect-related absorption may compete with $Yb^{3+}$ CT absorption causing the dip clearly revealed at around 6.7 eV in the excitation spectrum of $Yb^{3+}$ CTL for the $LiY_{0.9}Yb_{0.1}P_4O_{12}$ sample (figure 3(a), curve 1). The second maximum in the excitation spectrum of $Yb^{3+}$ CTL is observed at 7.35 eV (figure 3(a), curves 1, 2). It is more pronounced for the $LiY_{0.9}Yb_{0.1}P_4O_{12}$ sample (curve 1) and may appear due to the etching of the single CT absorption band (5.6–8.2 eV) by the defect-related absorption around 6.7 eV.

One may consider the excitation of $Yb^{3+}$ CTL in the 5.6–8.2 eV range to be due to the $Yb^{3+}$ CT absorption. However, the full width at half maximum (FWHM) of about 2 eV is rather large for a single $Yb^{3+}$ CT absorption band. For most Yb-doped materials the FWHM of CTL and CT absorption band have been found to be comparable, and the top of the valence band (VB) is consequently considered as the initial state for the charge transfer [9]. Perhaps for the case of the investigated $LiY_{1-x}Yb_xP_4O_{12}$ phosphates the electron transfer takes place not only from the levels near the top of the valence band but also from some deep VB levels. On the other hand, the FWHM of the first maximum (5.99 eV) in the excitation spectrum of $Yb^{3+}$ CTL (figure 3(a), curves 1, 2) is about 0.7 eV, being close to the FWHM ($\approx$0.8 eV) of the CTL emission bands (figure 1, curves 1, 2). The energy distance (1.35 eV) between two excitation peaks (5.99 and 7.35 eV; figure 3(a), curve 1) is larger by 0.11 eV than the splitting of the $Yb^{3+}$ $^2F$ term (1.24 eV). Here one can only suppose that the second maximum at 7.35 eV in the excitation spectra of $Yb^{3+}$ CTL (figure 3(a), curve 1) originates from electron transfer from the $O^{2-}$ ligand to $Yb^{3+}$ in the excited $^2F_{5/2}$ state. However, such an alternative explanation for the origin of the second 7.35 eV peak in the excitation spectra of $Yb^{3+}$ CTL has to be proved by further investigation. The absorption peak at 7.35 eV is possibly not well resolved for $LiY_{0.1}Yb_{0.9}P_4O_{12}$ (figure 3(a), curve 2) because the efficiency of the $Yb^{3+}$ $^2F_{5/2}$ state population is lower in this sample (figure 3(b), curve 2).

The excitation spectrum of $Yb^{3+}$ f–f emission plotted for the $LiY_{0.9}Yb_{0.1}P_4O_{12}$ sample (figure 3(b), curve 1) reproduces the features of the respective $Yb^{3+}$ CTL excitation spectrum (figure 3(a), curve 1) within the 8.2–10.5 eV range. Infrared $Yb^{3+}$ f–f emission is quite efficient for the $LiY_{0.9}Yb_{0.1}P_4O_{12}$ sample in the range of excitonic transitions, whereas its intensity decreases dramatically for $LiY_{0.1}Yb_{0.9}P_4O_{12}$ when the excitation energy exceeds 8.3 eV.

### *3.3. Excitonic mechanisms of excitation*

The excitation spectra of $Yb^{3+}$ CTL (figure 3(a), curves 1, 2) reproduce the peak of exciton absorption transitions at 8.55 eV revealed for a pure $LiYP_4O_{12}$ matrix (figure 3(b), curve 3). Two peaks at 8.36 eV and 8.43 eV appear as an extra feature for Yb-doped samples (figure 3(a), inset). The higher energy (8.43 eV) peak is not well resolved for the $LiY_{0.9}Yb_{0.1}P_4O_{12}$ sample (curve 1) due to overlap with the exciton absorption peak (8.55 eV) which is more intense compared to the case of $LiY_{0.1}Yb_{0.9}P_4O_{12}$ (curve 2).

The decay kinetics of $Yb^{3+}$ CTL registered for the $LiY_{0.9}Yb_{0.1}P_4O_{12}$ sample shows the rise component ($\tau_R = 9$ ns) upon excitation in the 8.36 eV peak (figure 4, curve 2). Such a rise effect is not revealed for the $LiY_{0.9}Yb_{0.1}P_4O_{12}$ sample upon excitation in the exciton transition peak (8.55 eV) (curve 3). The rise component ($\tau_R \approx 15$ ns) is also revealed for $LiY_{0.1}Yb_{0.9}P_4O_{12}$, but upon excitation in both 8.36 and 8.55 eV peaks (figure 4, curves 6, 7). The decay kinetics curves of $Yb^{3+}$ CTL are similar for $LiY_{0.1}Yb_{0.9}P_4O_{12}$ upon excitation in the 8.36, 8.55 eV peaks and reveal the same temperature dependence in the 8–320 K temperature range. This similarity may be considered as evidence for the excitonic nature of both 8.36 and

8.55 eV peaks in the $Yb^{3+}$ CTL excitation spectrum. The peak at 8.36 eV can be attributed to the near-activator exciton, and the rise component, revealed in the decay kinetics of $Yb^{3+}$ CTL upon excitation at 8.36 eV, may correspond to the formation of a $Yb^{2+}$ CT cluster due to the nonradiative decay of the near-activator exciton on the impurity $Yb^{3+}$ ion.

Thus, there is no time difference in the energy transfer from the regular ($E_{exc} = 8.55$ eV) or near-activator ($E_{exc} = 8.36$ eV) excitons to a $Yb^{3+}$ ion in the $LiY_{0.1}Yb_{0.9}P_4O_{12}$ sample due to the high concentration of $Yb^{3+}$ providing the small distance between impurity ions. Therefore, the value of the rise time $\tau_R$ constant is almost the same (about 15 ns) for $Yb^{3+}$ CTL of $LiY_{0.1}Yb_{0.9}P_4O_{12}$ upon excitation in the regular and near-activator exciton peaks (figure 4, curves 6, 7). For the $LiY_{0.9}Yb_{0.1}P_4O_{12}$ sample the time of migration of a regular exciton to $Yb^{3+}$ is longer because of the larger distance between $Yb^{3+}$ impurity ions. Therefore, the rise component is not revealed in the decay kinetics of $Yb^{3+}$ CTL for the $LiY_{0.9}Yb_{0.1}P_4O_{12}$ sample upon excitation in the regular exciton peak at 8.55 eV (figure 4, curve 3).

### *3.4. Fast decay component*

The short decay time of $Yb^{3+}$ CTL and the possible elaboration of fast Yb-doped scintillators have already been reported in [8] for example. The fast decay component (<1 ns) is also revealed for $Yb^{3+}$ CTL of $LiY_{1-x}Yb_xP_4O_{12}$ ($x = 0.1; 0.9$) samples upon excitation in the 8.3–17 eV range at $T = 8$ K (see figure 4). The only exception is the case of the $LiY_{0.9}Yb_{0.1}P_4O_{12}$ sample upon excitation in the regular exciton absorption (8.55 eV) peak (figure 4, curve 3), when most electrons are bounded with the localized holes forming regular self-trapped excitons (STE). The influence of the localization processes is reduced for the $LiY_{0.1}Yb_{0.9}P_4O_{12}$ sample due to the smaller distance between $Yb^{3+}$ impurity ions. The fast decay component is therefore more pronounced for $LiY_{0.1}Yb_{0.9}P_4O_{12}$ (figure 4, curves 6–8), being revealed even upon excitation in the regular exciton absorption (8.55 eV) peak (curve 7).

One may presume that the fast decay component of $Yb^{3+}$ CTL originates from the consequent recombination of a $Yb^{3+}$ ion with a free electron and hole. This recombination may give rise to a very fast emission since the probability of such collision processes is rather high for free carriers. Fast emission may also appear from the non relaxed or partly relaxed $Yb^{3+}$ CT states. The fast decay component of $Yb^{3+}$ CTL is better revealed for the $LiY_{0.1}Yb_{0.9}P_4O_{12}$ sample. However, the efficiency of CTL for $LiY_{0.1}Yb_{0.9}P_4O_{12}$ becomes about two times lower than one for $LiY_{0.9}Yb_{0.1}P_4O_{12}$ upon the excitation at $E_{exc} > 8.5$ eV (figure 3(a), curves 1, 2), whereas the respective efficiencies are almost equal in the 5.6–8.3 eV excitation range. The appearance of the fast decay component of $Yb^{3+}$ CTL that is observed together with a decrease in its efficiency for the $LiY_{0.1}Yb_{0.9}P_4O_{12}$ sample upon band-to-band excitation implies the quenching of $Yb^{3+}$ CTL. Thus, the fast component of $Yb^{3+}$ CTL decay is most likely caused by the nonradiative decay of $Yb^{3+}$ CT excited states.

The fast component of $Yb^{3+}$ CTL decay may result from the recombination of free carriers with a $Yb^{2+}$ CT cluster. Due to the smaller distance between impurity $Yb^{3+}$ ions in $LiY_{0.1}Yb_{0.9}P_4O_{12}$ the free carriers have a higher probability of recombining with the hole or electron involved into a $Yb^{2+}$ CT cluster, and in this way cause the fast decay of $Yb^{3+}$ CTL. In the case of the $LiY_{0.9}Yb_{0.1}P_4O_{12}$ sample the recombination of $Yb^{2+}$ CT clusters with free carriers is reduced since most electrons are bounded with localized holes forming regular self-trapped excitons. Therefore: (i) the efficiency of $Yb^{3+}$ CTL is higher for $LiY_{0.9}Yb_{0.1}P_4O_{12}$ (figure 3(a), curve 1) in comparison with $LiY_{0.1}Yb_{0.9}P_4O_{12}$ (figure 3(a), curve 2) at $E_{exc} > 8.5$ eV, (ii) the fast decay component is absent for the $LiY_{0.9}Yb_{0.1}P_4O_{12}$ sample upon excitation at 8.55 eV (figure 4, curve 3) and (iii) its contribution at $E_{exc} = 15.69$ eV is lower (curve 4) than for $LiY_{0.1}Yb_{0.9}P_4O_{12}$ (curve 8).

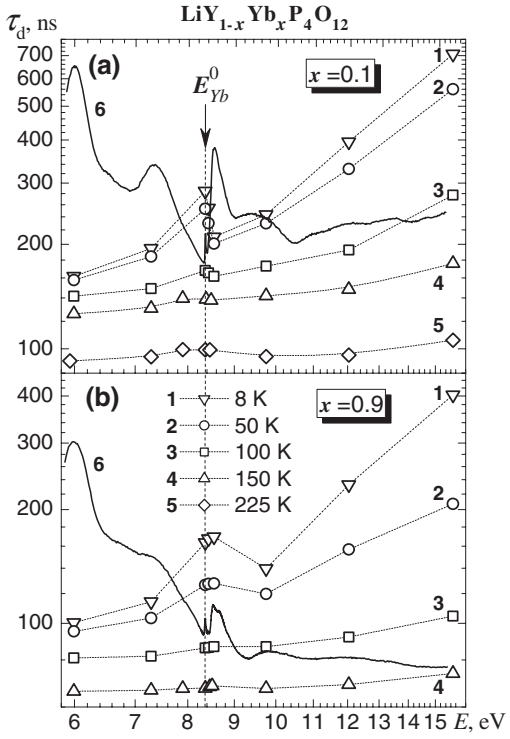


**Figure 5.** Dependence of the decay time of $Yb^{3+}$ CT emission of $LiY_{1-x}Yb_xP_4O_{12}$ ($x = 0.1$; 0.9) on the energy of excitation quanta in the temperature range 8–320 K.

### *3.5. High-energy excitation*

In the case of the high-energy excitation $E_{exc} > E_g + E_{CT} \approx 15$ eV the CT states of $Yb^{3+}$ can be formed due to electron impact. The impact excitation mechanism is possible when fast photoelectrons in the conduction band excite the emission centres directly (via impact) [20]. Such impact excitation should be more efficient for the case of higher impurity concentrations [20]. However, the expected increase of $Yb^{3+}$ CTL efficiency upon the excitation of $LiY_{0.1}Yb_{0.9}P_4O_{12}$ sample at $E_{exc} > E_g + E_{CT} \approx 15$ eV (figure 5(b), curve 6) may possibly be completely annihilated by the nonradiative decay of $Yb^{3+}$ CT states due to the recombination of a free electron with the hole involved into a $Yb^{2+}$ CT cluster.

Thus, upon excitation within the energy range of band-to-band transitions the relaxation of free electrons causes the formation of (i) $Yb^{2+}$ CT clusters due to the electron impact ($E_{exc} > E_g + E_{CT} \approx 15$ eV) and a (ii) $Yb^{2+}$ ion after electron recombination with a $Yb^{2+}$ CT cluster (causes the fast decay of CTL). Hole thermalization may result in the formation of a $Yb^{2+}$ CT cluster after hole localization around a $Yb^{2+}$ ion, but formation of a self-trapped exciton is most probable for the case of a small concentration of $Yb^{3+}$ impurities. Exciton decay on the impurity $Yb^{3+}$ ion may also result in the formation of $Yb^{3+}$ CT excited state, but for this case the decay time increases and the rise component may appear in the decay kinetics of $Yb^{3+}$ CTL.

The considerable difference in the slow decay components of $Yb^{3+}$ CTL is observed for $LiY_{0.9}Yb_{0.1}P_4O_{12}$ ($\tau_d = 760$ ns) and $LiY_{0.1}Yb_{0.9}P_4O_{12}$ ($\tau_d = 400$ ns) samples upon excitation at 15.69 eV (figure 4, curves 4 and 8, respectively). The efficiency of formation of $Yb^{2+}$ is rather high for the $LiY_{0.1}Yb_{0.9}P_4O_{12}$ sample at $E_{exc} = 15.69$ eV due to the impact excitation accompanied by nonradiative $Yb^{2+}$ CT cluster decay (cluster recombination with

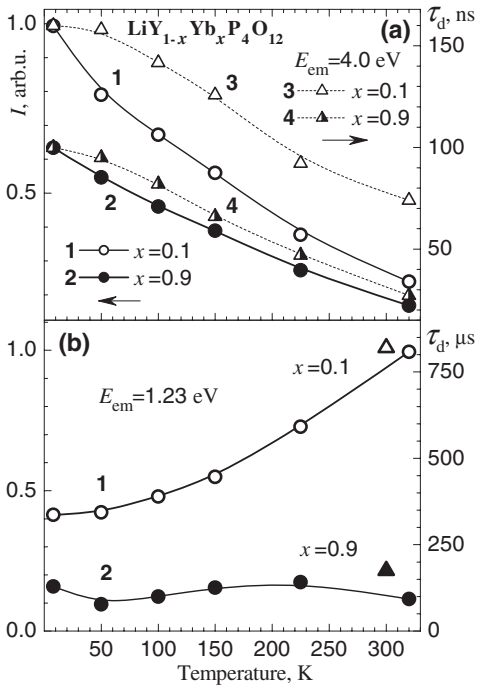


**Figure 6.** Temperature dependences of (a) $Yb^{3+}$ CTL efficiency (curves 1, 2, resulted from the integration of excitation spectra in 5.5–17 eV range) and decay time (curves 3, 4) upon $E_{exc} = 5.99$ eV; (b) decay time (triangles) and intensity of infrared $Yb^{3+}$ f–f emission (circles) excited at $E_{exc} = 5.99$ eV.

a free electron). Thus, the slow component (400 ns) of $Yb^{3+}$ CTL decay registered for the $LiY_{0.1}Yb_{0.9}P_4O_{12}$ sample upon excitation at 15.69 eV (figure 4, curve 8) mostly characterizes the processes of hole migration and hole localization around the $Yb^{2+}$ ion. The respective decay kinetics of the $LiY_{0.9}Yb_{0.1}P_4O_{12}$ sample (figure 4, curve 4) has a more complex profile and reveals a larger (760 ns) time constant for the slow decay component since both the electrons and holes are involved in energy transfer from the host to the impurity $Yb^{3+}$ ion.

### *3.6. Temperature dependence*

Dependence of the decay time constant of $Yb^{3+}$ CTL on the excitation energy has been examined in the temperature range 8–225 K for the $LiY_{0.9}Yb_{0.1}P_4O_{12}$ sample (figure 5(a)) and within the 8–150 K range for $LiY_{0.1}Yb_{0.9}P_4O_{12}$ (figure 5(b)). The time constant increases while the energy of excitation quanta is changed from 6 eV up to 16 eV. An extra increase in the decay time constant is observed for the $LiY_{0.9}Yb_{0.1}P_4O_{12}$ sample upon excitation in the 8.36 eV peak corresponding to near-activator exciton formation. In the case of the $LiY_{0.1}Yb_{0.9}P_4O_{12}$ sample such an extra increase is observed upon excitation in both the near-activator (8.36 eV) and the regular (8.55 eV) exciton-related peaks. The general increase in the decay time for the higher excitation energies shows the delay in energy transfer from the host to the impurity $Yb^{3+}$ ion at low temperatures. Carrier trapping is reduced at higher temperatures and the decay time upon $E_{exc} = 6$–16 eV appears to be almost constant, being about 100 ns for $LiY_{0.9}Yb_{0.1}P_4O_{12}$ at 225 K (figure 5(a), curve 5) and 65 ns for $LiY_{0.1}Yb_{0.9}P_4O_{12}$ already at 150 K (figure 5(b), curve 4).

Temperature dependences of the decay time and the efficiency of $Yb^{3+}$ CTL are presented for both Yb-doped samples in figure 6(a). To plot the efficiency dependences (curves 1, 2) integration of the CTL excitation spectra was performed within the 5.5–17 eV range

for each temperature in order to include the recombinational mechanisms of excitation. Dependences of the decay time constant (curves 3, 4) are presented only for the excitation of the $Yb^{3+}$ CTL in the CT absorption peak (5.99 eV). In this way two quenching temperatures, ${}^{I}T_q$ and ${}^{\tau}T_q$, have been estimated from the dependences of efficiency and decay time, respectively. The temperature values at corresponding half-maxima have been considered for this purpose. A large difference between ${}^{I}T_q$ (175 K) and ${}^{\tau}T_q$ (290 K) has been revealed for the $LiY_{0.9}Yb_{0.1}P_4O_{12}$ sample due to the exciton thermal decay up to 180 K. The contribution from the recombinational excitation of $Yb^{3+}$ CTL is reduced when the concentration of impurity $Yb^{3+}$ ions is higher (figure 5(b), curve 6). Therefore, the value of ${}^{I}T_q$ (205 K) is not too different from ${}^{\tau}T_q$ (215 K) for the $LiY_{0.1}Yb_{0.9}P_4O_{12}$ sample. The thermostimulated decay of the $Yb^{2+}$ CT cluster is characterized by the parameter ${}^{\tau}T_q$ corresponding to excitation directly in the CT absorption peak (5.99 eV). Therefore, the quenching temperature of the $Yb^{3+}$ CTL has been estimated to be about 290 K and 215 K for $LiY_{0.9}Yb_{0.1}P_4O_{12}$ and $LiY_{0.1}Yb_{0.9}P_4O_{12}$ samples, respectively. The lower quenching temperature (215 K) for the $LiY_{0.1}Yb_{0.9}P_4O_{12}$ sample is most likely caused by the intensification of interaction between $Yb^{2+}$ CT clusters due to the smaller distance between $Yb^{3+}$ impurity ions.

The temperature dependence of the intensity of infrared $Yb^{3+}$ f–f emission excited in the $Yb^{3+}$ CT absorption peak (5.99 eV) is presented in figure 6(b) (curves 1, 2). As the temperature goes up from 8 K up to 320 K, the intensity of infrared $Yb^{3+}$ f–f emission increases more than twice for the $LiY_{0.9}Yb_{0.1}P_4O_{12}$ sample (curve 1) but remains almost constant for $LiY_{0.1}Yb_{0.9}P_4O_{12}$ (curve 2). Such changes in the temperature dependence of $Yb^{3+}$ f–f emission efficiency with concentration (figure 6(b), curves 1, 2) may be explained by different mechanisms of $Yb^{2+}$ CT cluster decay dominating for $LiY_{0.9}Yb_{0.1}P_4O_{12}$ and $LiY_{0.1}Yb_{0.9}P_4O_{12}$ samples. At the lower concentration of impurity $Yb^{3+}$ ions both the electron and the hole may escape from the $Yb^{2+}$ CT cluster. The $Yb^{3+}$ ion appearing in this way may still be in the ${}^2F_{5/2}$ excited state and $Yb^{3+}$ f–f emission is observed for this case. There should be no possibility of observing $Yb^{3+}$ f–f emission when the decay of the $Yb^{2+}$ CT cluster appears mostly due to hole escape and consequent formation of $Yb^{2+}$ ions. An increase in the impurity concentration of $Yb^{3+}$ reduces the distance between $Yb^{3+}$ ions. Therefore, in the case of $LiY_{0.1}Yb_{0.9}P_4O_{12}$ the cross-recombination of electrons and holes from the different $Yb^{2+}$ CT clusters may be thermally stimulated, thus implying the appearance of $Yb^{2+}$ and a reduced probability of occurrence of $Yb^{3+}$ ${}^2F_{5/2}$. Such cross-recombination may be the reason for the low efficiency of infrared $Yb^{3+}$ f–f emission in the $LiY_{0.1}Yb_{0.9}P_4O_{12}$ sample upon excitation at $E > 8.3$ eV, even at $T = 8$ K (figure 3(b), curve 2).

The value of the intensity ratio for $Yb^{3+}$ f–f emission is roughly reproduced by its decay time constants measured for $LiY_{0.9}Yb_{0.1}P_4O_{12}$ (820 $\mu$s) and $LiY_{0.1}Yb_{0.9}P_4O_{12}$ (175 $\mu$s) at $T = 300$ K upon direct f–f excitation (figure 6(b), triangles). The decay kinetics for $Yb^{3+}$ f–f emission was measured using an optical parametric oscillator OPO LP 601 from SOLAR Laser Systems (Minsk, Belarus) as an excitation source. The excitation wavelength $\lambda_{exc}$ was about 975 nm (i.e. into the O-phonon line) and was adjusted for the maximum fluorescence signal at $\lambda_{em} = 1020$ nm. The duration of the excitation pulse $\delta t$ was about 6 ns. A series of glycerin solutions (down to 0.3 wt%) of Yb-doped powders were studied in order to suppress the reabsorption resulting in decay delay. The minimum decay time constant was reached at 0.5 wt% for the $LiY_{0.1}Yb_{0.9}P_4O_{12}$ sample and at 1 wt% for the $LiY_{0.9}Yb_{0.1}P_4O_{12}$.

## 4. Conclusions

When discussing the relaxation of the $Yb^{3+}$ CT state one should take into account that after charge transfer occurs $RE^{2+}$ is formed and $4f^n$ states of $RE^{3+}$ can be realized only after $RE^{2+}$

CT cluster decay via electron escape from $RE^{2+}$ or its recombination with the hole localized on the ligand.

The excited $Yb^{3+}$ CT state may appear after:

- electron transfer from the surrounding ligand to a $Yb^{3+}$ ion;
- exciton decay on the impurity $Yb^{3+}$ ion;
- hole localization around the $Yb^{2+}$ ion;
- electron impact ($E_{exc} > E_g + E_{CT}$).

The fast decay component of $Yb^{3+}$ CTL upon band-to-band excitation may be caused by the quenching of $Yb^{3+}$ CTL due to the recombination of free carriers with the hole or electron involved in the $Yb^{2+}$ CT cluster. This quenching mechanism comes to be more pronounced for $LiY_{1-x}Yb_xP_4O_{12}$ when the impurity concentration increases.

A thermostimulated increase of infrared $Yb^{3+}$ f–f emission intensity may be observed in the case of $Yb^{2+}$ CT cluster decay via the escape of an electron from $Yb^{2+}$ or its recombination with the hole localized on a ligand around $Yb^{2+}$. When a $Yb^{2+}$ CT cluster decays due to the escape of its hole component then $Yb^{2+}$ ion formation reduces the probability of the appearance of $Yb^{3+}$ $^2F_{5/2}$ and the intensity of $Yb^{3+}$ f–f emission is low. Impurity concentration may influence the dominant mechanism of $Yb^{2+}$ CT cluster decay. For a high-concentration system the cross-recombination of electrons and holes from the different $Yb^{2+}$ CT clusters may occur leading to formation of $Yb^{2+}$.

Let us consider the possible relaxation processes in materials doped with a trivalent $A^{3+}$ ion. Upon excitation in the $A^{3+}$ CT absorption band the transfer of an electron from ligands (i.e. from the valence band) to a trivalent $A^{3+}$ impurity ion takes place and a mobile hole remains in the valence band. Further behaviour of this hole defines the relaxation processes that may result in the appearance of the three following types of luminescence:

(1) $e^- + A^{3+} \rightarrow (A^{2+})^* \rightarrow A^{2+}+$ emission characteristic for the $A^{2+}$ centres;
(2) $e^- + A^{3+} \rightarrow \{A^{2+}, V_K\} \rightarrow A^{3+}ex^o \rightarrow A^{3+}+$ the emission of an exciton localized near $A^{3+}$;
(3) $e^- + A^{3+} \rightarrow A^{3+}e^- = A^{2+} \cdots e_L^+ \rightarrow A^{3+}+$ the CT luminescence.

$(A^{2+})^*$—excited state of $A^{2+}$ ion;
$\{A^{2+}, V_K\}$—self-trapped hole ($V_K$-centre) near $A^{2+}$ ion;
$A^{3+}ex^o$—exciton localized near $A^{3+}$;
$A^{2+} \cdots e_L^+$—hole distributed over the ligands around $A^{2+}$ ion.

In all these cases the optically released electron is trapped by the impurity $A^{3+}$ ion. Thus, the probabilities of these three processes depend mainly on the behaviour of the optically released hole in the material studied: (1) immediate self-trapping of the hole or its trapping at some defect; (2) fast migration of a mobile hole along the lattice and its self-trapping close to an electron impurity centre $A^{2+}$; (3) delocalization of the hole over ligands around the electron impurity $A^{2+}$ centre.

Process (1) is the trapping of an electron by the impurity $A^{3+}$ ion or the recombination of an electron with the $A^{3+}$ ion. This process can be realized under excitation in the charge transfer absorption band only in the case when the optically released mobile holes are immediately self-trapped in the crystal lattice or trapped by some defects, i.e. in the case when the holes are removed from the process. As a result of this process, the same emission appears as that observed under direct excitation in the absorption bands of the $A^{2+}$ centre. Process (2) is similar to that observed, e.g., in CsI:Tl [21] and results in the appearance of localized exciton luminescence. In this case both the electron and the hole take part in the process. For that, the probability of recombination of an electron from an $A^{2+}$ ion with the hole self-trapped close

to the electron $A^{2+}$ centre should be large enough. Only process (3) results in the creation of the CT excited state, where the electron is located at $A^{3+}$ and the hole ($e_L^+$) is localized at the ligands around $A^{2+}$. The electron transition from $A^{2+}$ to $e_L^+$ results in the appearance of the CT luminescence.

In some systems there may be the competition between the processes mentioned above. The CT luminescence should be intense in the systems where process (3) is preferable to processes (1) and (2), i.e. where the self-trapping of holes is not possible and where an $A^{3+}$ ion prefers to take an electron from the valence band, but the electron is not bonded very strongly with the $A^{3+}$ ion (i.e. the $A^{2+}$ centre is not too stable) and prefers to return to $e_L^+$. In this case the hole cannot be self-trapped and it cannot recombine immediately with the electron but prefers to be distributed over all the ligands around the impurity ion. This means that the ligands should be able to keep the hole at some distance from the electron located at $A^{3+}$. The state of the hole ($e_L^+$) delocalized at the ligands should be far enough from the top of the valence band (VB) to avoid the escape of the hole to the VB [5, 22] and thermal quenching of the CT luminescence at very low temperatures. For that, the relaxation of the hole state should be large enough. The energy distance between the top of the valence band and the $e_L^+$ level increases with increasing hole binding energy, i.e. (1) as the lattice constant increases, (2) as the polarizability of the nearest neighbouring anions decreases, and (3) as the size of the substituting host cation increases (in isostructural compounds with the same anions). The thermally stimulated nonradiative transitions from the excited CT state to the $4f^n$ ground state of $RE^{3+}$ [22] may also be responsible for the strong quenching of the CT luminescence.

## References


[1] Raghavan R S 1997 *Phys. Rev. Lett.* **78** 3618
[2] Nakazawa E 1978 *Chem. Phys. Lett.* **56** 161
[3] Nakazawa E 1979 *J. Lumin.* **18/19** 272
[4] Danielson E *et al* 1998 *Science* **279** 837
[5] van Pieterson L, Heeroma M, de Heer E and Meijerink A 2000 *J. Lumin.* **91** 177
[6] Kamenskikh I A *et al* 2003 *Opt. Mater.* **24** 267
[7] Kamenskikh I A *et al* 2005 *J. Phys.: Condens. Matter* **17** 5587
[8] Nikl M *et al* 2004 *Appl. Phys. Lett.* **84** 882
[9] Dorenbos P 2003 *J. Phys.: Condens. Matter* **15** 8417
[10] Guerassimova N, Garnier N, Dujardin C, Petrosyan A G and Pedrini C 2001 *J. Lumin.* **94/95** 11
[11] Chipaux R *et al* 2002 *Nucl. Instrum. Methods Phys. Res.* A **486** 228
[12] Antonini P, Bressi G, Carugno G and Iannuzzi D 2001 *Nucl. Instrum. Methods Phys. Res.* A **460** 469
[13] Adachi H, Tsukada M and Satoko C 1978 *J. Phys. Soc. Japan* **45** 875
[14] Rodnyi P A 1992 *Sov. Phys.—Solid State* **34** 1053
[15] Ikeda T, Kobayashi H, Ohmura Y, Nakamatcu H and Mukoyama T 1997 *J. Phys. Soc. Japan* **66** 1079
[16] Shionoya S and Yen W M 1999 *Phosphore Handbook* (New York: CRC Press) pp 180–4
[17] Danielmayer H G and Weber H P 1972 *IEEE J. Quantum. Electron.* **8** 805
[18] Voloshinovskii A S *et al* 2003 *HASYLAB Annual Report 2002* p 445
[19] Zimmerer G 1991 *Nucl. Instrum. Methods* A **308** 178
[20] Makhov V N *et al* 2000 *J. Lumin.* **87–89** 1005
[21] Babin V, Kalder K, Krasnikov A and Zazubovich S 2002 *J. Lumin.* **96** 75
[22] van Pieterson L 2001 Charge transfer and $4f^n$–$4d^{n-1}5d$ luminescence of lanthanide ions *PhD Thesis* Utrecht University